Genetic Defects in Human Pericentrin Are Associated With Severe Insulin Resistance and Diabetes

Isabel Huang-Doran,[1] Louise S. Bicknell,[2] Francis M. Finucane,[3] Nuno Rocha,[1] Keith M. Porter,[1] Y.C. Loraine Tung,[1] Ferenc Szekeres,[4] Anna Krook,[4] John J. Nolan,[3] Mark O'Driscoll,[5] Michael Bober,[6] Stephen O'Rahilly,[1] Andrew P. Jackson,[2] and Robert K. Semple,[1] for the Majewski Osteodysplastic Primordial Dwarfism Study Group*

OBJECTIVE—Genetic defects in human pericentrin (*PCNT*), encoding the centrosomal protein pericentrin, cause a form of osteodysplastic primordial dwarfism that is sometimes reported to be associated with diabetes. We thus set out to determine the prevalence of diabetes and insulin resistance among patients with *PCNT* defects and examined the effects of pericentrin depletion on insulin action using 3T3-L1 adipocytes as a model system.

RESEARCH DESIGN AND METHODS—A cross-sectional metabolic assessment of 21 patients with *PCNT* mutations was undertaken. Pericentrin expression in human tissues was profiled using quantitative real-time PCR. The effect of pericentrin knockdown on insulin action and adipogenesis in 3T3-L1 adipocytes was determined using Oil red O staining, gene-expression analysis, immunoblotting, and glucose uptake assays. Pericentrin expression and localization also was determined in skeletal muscle.

RESULTS—Of 21 patients with genetic defects in *PCNT*, 18 had insulin resistance, which was severe in the majority of subjects. Ten subjects had confirmed diabetes (mean age of onset 15 years [range 5–28]), and 13 had metabolic dyslipidemia. All patients without insulin resistance were younger than 4 years old. Knockdown of pericentrin in adipocytes had no effect on proximal insulin signaling but produced a twofold impairment in insulin-stimulated glucose uptake, approximately commensurate with an associated defect in cell proliferation and adipogenesis. Pericentrin was highly expressed in human skeletal muscle, where it showed a perinuclear distribution.

CONCLUSIONS—Severe insulin resistance and premature diabetes are common features of *PCNT* deficiency but are not congenital. Partial failure of adipocyte differentiation may contribute to this, but pericentrin deficiency does not impair proximal insulin action in adipocytes. ***Diabetes*** **60:925–935, 2011**

From the [1]Institute of Metabolic Science, Addenbrooke's Hospital, University of Cambridge Metabolic Research Laboratories, Cambridge, U.K.; the [2]Medical Research Council Human Genetics Unit, Institute of Genetics and Molecular Medicine, Western General Hospital, Edinburgh, U.K.; the [3]Metabolic Research Unit, St. James Hospital, Trinity College, Dublin, Ireland; [4]Integrative Physiology, Department of Physiology and Pharmacology, Karolinska Institute, Stockholm, Sweden; the [5]Human DNA Damage Response Disorders Group, University of Sussex, Brighton, U.K.; and the [6]Division of Genetics, Department of Pediatrics, Alfred I. DuPont Hospital for Children, Wilmington, Delaware.

Corresponding author: Robert K. Semple, rks16@cam.ac.uk.

Received 18 September 2010 and accepted 13 December 2010.

DOI: 10.2337/db10-1334

This article contains Supplementary Data online at http://diabetes.diabetesjournals.org/lookup/suppl/doi:10.2337/db10-1334/-/DC1.

*A complete list of the members of the Majewski Osteodysplastic Primordial Dwarfism Study Group can be found in the APPENDIX.

Insulin resistance is at pandemic levels and is associated with major mortality and morbidity predominantly attributed to atherosclerosis, microvascular complications of diabetes, hepatic steatosis, and polycystic ovary syndrome (1). Pandemic insulin resistance is likely to be accounted for by an oligogenic diathesis interacting with environmental factors, by far the most important of which is obesity (2,3). However, studies to date have identified only a handful of common genetic variants plausibly associated with insulin resistance risk, collectively accounting for only a small proportion of the insulin resistance in the general population (4–6).

We have adopted a complementary strategy to population-wide genetic approaches, first by identifying single-gene defects in rare patients with unusually severe insulin resistance and then by comparing and contrasting their perturbed physiology with that of prevalent forms of insulin resistance. In a large cohort of patients with extreme insulin resistance, we identified two patients with osteodysplastic primordial dwarfism of Majewski type 2 (MOPDII; MIM 210720), recently shown to be caused by mutations in the *PCNT* gene (7,8). *PCNT* encodes pericentrin, a 360-kDa coiled-coil protein that localizes to the pericentriolar matrix throughout the cell cycle (9–12). This finding, together with scattered reports of early-onset diabetes and acanthosis nigricans in patients with clinical features of MOPDII, led us to study the prevalence and natural history of insulin resistance in patients with *PCNT* loss-of-function mutations (7,8,13). In addition, we used an in vitro approach to explore the role of pericentrin in insulin action. Using the 3T3-L1 adipocyte cell line as a model system, the effects of pericentrin deficiency on insulin responsiveness and adipocyte differentiation, both of which make key contributions to metabolic homeostasis in vivo, were assessed.

RESEARCH DESIGN AND METHODS

Patients with insulin resistance and MOPDII were identified as part of a long-standing program of research into severe insulin resistance. All physiological and genetic studies were approved by the National Health Service Research Ethics Committee of the U.K. Each participant provided written informed consent, and all studies were conducted in accordance with the principles of the Declaration of Helsinki. Additional patients with MOPDII and proven *PCNT* mutations underwent a basic metabolic evaluation as part of their routine clinical care.

Genetic studies. The sequence analysis of the *PCNT* gene has been described previously (7,8). Single nucleotide polymorphism genotyping and copy-number analysis of patient 2 and her father was undertaken using Affymetrix 6.0 chips, with data analyzed using the Affymetrix Genotyping Console (Santa Clara, CA).

Biochemical assays. Venous blood was drawn in the fasting state, and plasma was immediately extracted and stored at −20°C. Insulin, leptin, and

adiponectin were assayed using two-step time-resolved AutoDELFIA immunoassays, as previously described (14–16). All other analytes were determined in accredited clinical diagnostic laboratories of referring hospitals. For oral glucose tolerance testing, 1.75 g glucose/kg body wt was given after a 10-h fast, and blood samples were taken at the times indicated for determination of plasma glucose and insulin.

Body composition and abdominal fat measurement. Body composition was measured by Lunar Prodigy dual-energy X-ray absorptiometry (GE Lunar), and proton magnetic resonance spectroscopy (MRS) was undertaken using a Siemens 3T Tim Trio MR scanner and protocols described in detail previously (15).

Cell culture. All reagents were obtained from Sigma-Aldrich (St. Louis, MO), unless otherwise indicated. Cells were cultured in 100 units/L penicillin, 100 μg/mL streptomycin, and 2 mmol/L L-glutamine. Generation and culture of Epstein-Barr virus–transformed lymphoblastoid cell lines and dermal fibroblasts are described in the Supplementary Methods. Human embryonic kidney 293–BOSC packaging cells (Dr. J. Rochford, University of Cambridge) were maintained in DMEM with FBS (DMEM-FBS). Murine 3T3-L1 preadipocytes (American Tissue Culture Collection, Manassas, VA) were maintained below 70% confluence in DMEM with neonatal calf serum. To induce adipocyte differentiation, 2-day postconfluent preadipocytes were transferred to DMEM-FBS, supplemented with 500 μmol/L 3-isobutyl-1-methylxanthine (3 days), 1 μmol/L dexamethasone (3 days), 10 μmol/L insulin (6 days; Novo Nordisk; Bagsværd, Denmark), and 100 nmol/L rosiglitazone (6 days). Experiments were performed 10 days after inducing differentiation. Differentiation was assessed by staining formalin-fixed adipocytes with 1.5 mmol/L Oil-Red-O in isopropanol (17). For proliferation studies, cell numbers were quantified using the CyQuant Cell Proliferation assay (Invitrogen, Carlsbad, CA).

Short-hairpin RNA–mediated pericentrin knockdown. Short-hairpin RNA (shRNA) constructs targeting murine *Pcnt* (NM_008787) (shPcnt1: 5′-AATGAGGTTGTCCACAGGAGA-3′; shPcnt2: 5′-CGGTCTTGTGGAACCAGAA-3′) and firefly luciferase as a control (*shLuc*) were cloned into the RNA-Ready pSIREN-RetroQ Vector (Clontech, Palo Alto, CA). Infectious retroviruses were generated in BOSC-293 cells before infection of 3T3-L1 preadipocytes (Supplementary Methods) (17).

Gene-expression analysis. A commercial human-tissue RNA panel was obtained from AMS Biotechnology (Abingdon, U.K.); the murine-tissue RNA panel was a gift from Dr. Giles Yeo (University of Cambridge). Total RNA was extracted from cells using the RNEasy kit (Qiagen). Reverse transcription was performed using Moloney murine leukemia virus reverse transcriptase, random hexamers, and deoxynucleotide triphosphates, as per the manufacturer's guidelines (Promega, Madison, WI). Real-time quantitative PCR used an ABI 7900 detection system (Applied Biosystems, Foster City, CA), a Taqman PCR Mastermix (Applied Biosystems), gene-specific forward and reverse primers, and 5′-[FAM], 3′[TAMRA]-labeled fluorogenic probes. Sequences or catalog numbers for all primers and probes used are listed in the Supplementary Material.

Western blotting. Cell lysis was performed as described previously (18). Protein concentrations were determined using the Bio-Rad D_c Protein Assay (Bio-Rad, Hercules, CA). Proteins were denatured at 95°C then resolved by SDS-PAGE and transferred to polyvinylidene fluoride membranes using the iBlot system (Invitrogen). Membranes were blocked in 5% milk before immunoblotting. Sources of all primary antibodies are listed in the Supplementary Material. Horseradish peroxide–conjugated secondary antibodies were obtained from Thermo Pearce and visualized using an enhanced chemoluminescence system (GE Healthcare).

Deoxyglucose uptake assay. Serum-starved adipocytes were exposed to 100 nmol/L insulin or PBS in glucose-free HEPES buffer for 30 min followed by incubation in 1 μCi/mL [^{3}H]deoxyglucose for 5 min. Cells were lysed in 0.5 mol/L potassium hydroxide, neutralized in 0.5 mol/L hydrochloric acid, and intracellular ^{3}H was measured using Hionic-Fluor scintillant (Perkin Elmer) in a Tri-Carb 2100-TR Liquid Scintillation Analyzer (Packard). Radioactivity was normalized to protein concentration, which was determined using the Coomassie Plus Protein Assay (Thermo-Fisher Scientific).

Immunocytochemistry and immunohistochemistry. Cells grown on glass cover slips were fixed in ice-cold methanol or 3–4% neutral-buffered formaldehyde, followed by permeabilization in 0.5% saponin. Vastus lateralis biopsies were obtained from healthy volunteers (19), sectioned at −23°C, dried, and then fixed for 20 min in acetone at room temperature. All samples were blocked in 1% BSA before antibody treatment. Sources of all primary and secondary antibodies are listed in the Supplementary Material. Cells were mounted in ProLong Gold Antifade with DAPI (Invitrogen) and viewed using a Zeiss LSM510 MetaLaser Scanning Microscope (Carl Zeiss, Jena, Germany).

Statistical analysis. Differences in gene expression or glucose uptake between multiple groups or at different time points were evaluated by ANOVA with post hoc Bonferroni tests. Differences in cell proliferation rates were assessed by fitting linear regression lines then testing for gradient equality. All analyses were performed in GraphPad Prism 5.0 (GraphPad Software, San Diego, CA).

RESULTS

Early-onset, progressive insulin resistance in patients with *PCNT* defects. As part of a long-running program of investigation of severe insulin resistance, two patients were identified with severe insulin resistance as well as clinical features of MOPDII, as summarized in the Supplementary Results. Patient 1 (patient 23 in Rauch et al. [8]), a 29-year-old man, had compound heterozygous nonsense mutations in *PCNT*, with a 60% reduction in *PCNT* mRNA levels, loss of punctate juxtanuclear pericentrin immunostaining, and disorganization of the microtubule network in dermal fibroblasts. Pericentrin protein expression was nearly absent in Epstein-Barr virus–transformed lymphoblastoid cells (Supplementary Fig. 2). Patient 2 (patient 20 in Rauch et al. [8]), a 10-year-old girl, had a homozygous nonsense mutation in *PCNT* attributed to uniparental inheritance of the terminal part of chromosome 21 harboring a heterozygous mutation in her mother (Supplementary Fig. 4).

Patient 1. During evaluation of retarded growth at 3 years old, 0.016 units insulin/kg body wt produced an adequate hypoglycemia and growth-hormone response, suggesting no severe insulin resistance. A 6-month trial of growth hormone followed but was stopped because of inefficacy. At age 7 years, hypothyroidism was diagnosed and L-thyroxine replacement was started. At age 12 years, a centripetal distribution of adiposity associated with acanthosis nigricans was first noted. At age 15 years, testosterone replacement was commenced because of arrested puberty.

From age 21 years, severe acanthosis nigricans prompted serial metabolic evaluations that showed consistent extreme insulin resistance, severe mixed dyslipidemia, and, ultimately, diabetes at age 23 years (Table 1). Over the subsequent 4 years, good metabolic control was achieved on metformin and fenofibrate before the addition of rosiglitazone at age 28 years, when HbA_{1c} was 8.5%.

On examination at the age of 29 years, patient 1 was of extremely short stature, with characteristic dysmorphic features of MOPDII and a centripetal pattern of adiposity; however, although he had a relative paucity of adipose tissue on his legs, there was no frank lipodystrophy. There was florid acanthosis nigricans in the axillae, periumbilical region, antecubital fossae, groin, and neck. He was normally androgenized with androgenic alopecia, and his blood pressure was 100/55 mmHg. Oral glucose tolerance testing confirmed severely insulin-resistant diabetes and dyslipidemia (Tables 1 and 2). Adiponectin was severely suppressed, whereas leptin was slightly above the age- and BMI-adjusted normal range. Body composition analysis showed pronounced centripetal fat distribution, and MRS revealed hepatic steatosis (Table 2).

Clinical assessment and genotyping of the extended family of patient 1 provided no evidence that heterozygotes for either of the truncating mutations had reduced height or insulin sensitivity compared with family members wild-type for *PCNT* (Supplementary Fig. 1, Supplementary Table 3).

Patient 2. At age 4 years, patient 2 was evaluated for severe growth retardation, which led to the commencement of growth-hormone therapy at age 4.2 years. Despite dose titration to 0.5 mg/day, growth velocity remained poor, and IGF-1 at age 6.4 years remained low (18 nmol/L [normal range 24–46]). At age 8.9 years, centripetal weight

TABLE 1
Serial oral glucose tolerance testing in patient 1

	Age (years)						
	21		22.8		29		
	Treatment						
	NIL		NIL		500 mg metformin, 2 mg rosiglitazone, 200 mg fenofibrate		
Time (min)	Glucose (mg/dL)	Insulin (pmol/L)	Glucose (mg/dL)	Insulin (pmol/L)	Glucose (mg/dL)	Insulin (pmol/L)	Free fatty acids (μmol/L)
0	72	1,990	191	2,640	114	132	327
30	189	13,900	306	4,010	220	559	
60	229	18,900	384	4,700	279	1,260	251
90	202	19,900	411	6,770	308	1,550	
120	207	23,000	436	11,100	295	1,900	143
Fasting reference range	68–100	<60	68–100	<60	68–100	<60	

gain and severe acanthosis nigricans were noted. Laboratory studies showed a normal HbA_{1c} (6%) but elevated IGF-1 (75 nmol/L) and marked dyslipidemia (cholesterol 243 mg/dL, triglycerides 286 mg/dL) (Table 3). As a result, growth-hormone therapy was stopped with no discernible decline in growth velocity.

Two months later (at age 9.1 years), fasting glucose was normal but acanthosis nigricans and dyslipidemia had worsened (cholesterol 309 mg/dL, triglycerides 912 mg/dL) (Table 3). There was mildly deranged liver function (67 units/L alanine aminotransferase [ALT]), and ultrasonography showed hyperechoic echotexture of the liver, consistent with steatosis. Four months after cessation of growth-hormone therapy (at age 9.2 years), lipids remained elevated but had improved (cholesterol 212 mg/dL, triglycerides 221 mg/dL). Fasting hyperinsulinemia was noted, but there was no impaired glucose tolerance (Table 3). IGF-1 levels had normalized (34 nmol/L). However, on investigation at

TABLE 2
Metabolic evaluation of patients 1 and 2

	Patient 1	Patient 2	Fasting reference range
Age at evaluation (years)	29.0	10.7	
Sex	Male	Female	
Therapy	500 mg metformin, 2 mg rosiglitazone, 200 mg fenofibrate	500 mg metformin	
Height (m)	1.11	1.09	
Weight (kg)	28.7	24.3	
BMI (kg/m^2)	23.3	20.5	18.5–25
Waist-to-hip ratio	0.86	1.00	
HbA_{1c} (%)	9.1	5.6	8.0–13.2
Total cholesterol (mg/dL)	251.0	196.9	<200
Triglycerides (mg/dL)	486.7	300.9	<177
HDL cholesterol (mg/dL)	11.2	52.1	>39
LDL cholesterol (mg/dL)	ND	86.9	<130
Adiponectin (mg/L)	1.1	1.1	*
Leptin (μg/L)	9.7	28.1	*
SHBG (nmol/L)	13	9	†
IGFBP1 (ng/mL)	29.5	4.1	10–120
γGT (units/L)	61	233	0–33
ALT (units/L)	27	98	0–50
Dual-energy X-ray absorptiometry data			
Percentage fat (SD score)	21.8 (−0.72)	33.6 (0.24)	
Percentage fat (arms)	18.5	32.5	
Percentage fat (legs)	14.9	28.4	
Percentage fat (trunk)	26.7	38.7	
Percentage android	34.4	46.8	
MRS data			
Percentage fat (liver)	7.9	ND	

SD scores for percentage fat were derived from published data from age- and sex-matched control populations (29). *Reference ranges for leptin and adiponectin are dependent on sex and body weight. The relevant sex- and BMI-adjusted 95% population ranges for leptin and adiponectin are 0.4–8.3 μg/L and 2.6–12.6 mg/L, respectively, for patient 1 and 2.4–24.4 μg/L and 4.4–17.7 mg/L, respectively, for patient 2. †Reference ranges for SHBG are dependent on sex. Relevant ranges are 15–48 nmol/L for patient 1 and 26–110 nmol/L for patient 2. γGT, γ glutamyltransferase; FHS, follicle-stimulating hormone; LH, luteinizing hormone; ND, not done; TSH, thyroid-stimulating hormone.

TABLE 3
Serial metabolic assessment of Patient 2

	Age (years)								
	8.9	9.1	9.2		10.2		10.7		
	Treatment								
	Growth hormone (1 month)	Off growth hormone (2 months)	Off growth hormone (4 months)		Off growth hormone (15 months)		500 mg metformin; off growth hormone (21 months)		
Triglycerides (mg/dL) normal range <177	655	912	221		248		451		
Cholesterol (mg/dL) normal range <200	243	309	212		205		131		
Time (min)	ND	ND	Glucose (mg/dL)	Insulin (pmol/L)	Glucose (mg/dL)	Insulin (pmol/L)	Glucose (mg/dL)	Insulin (pmol/L)	FFA (μmol/L)
0	ND	ND	81	306	85	133	76	183	846
30	ND	ND	153	>1230	ND	ND	204	3850	640
60	ND	ND	153	>1230	ND	ND	218	3750	235
90	ND	ND	124	>1230	ND	ND	225	4430	206
120	ND	ND	141	>1230	308	>1000	178	4910	171
Fasting reference range			68–100	<60	68–100	<60	68–100	<60	

ND, not done or data unavailable.

age 10.2 years, 15 months after cessation of growth hormone, serum liver indices and lipid profile remained deranged, and oral glucose tolerance testing showed severe hyperinsulinemia and diabetes (Table 3).

Metformin was commenced at age 10.2 years, and a more detailed endocrine assessment was undertaken 6 months later, almost 2 years after cessation of growth-hormone therapy. Physical examination revealed signs of early puberty (Tanner stage A1, P2, B2), pronounced acanthosis nigricans in the nuchal regions and axillae, centripetal fat distribution, and 2–3 cm palpable hepatomegaly but no lipodystrophy. Despite a normal HbA_{1c}, oral glucose tolerance testing again showed severe hyperinsulinemia, with persisting fasting dyslipidemia, relatively high leptin, and low adiponectin (Tables 2 and 3). ALT remained elevated, consistent with hepatic steatosis. Body composition analysis showed satisfactory bone-mineral density and centripetal fat distribution (Table 2).

Cross-sectional metabolic assessment of a cohort of patients with *PCNT* defects. In view of the severity of the insulin resistance in the two index patients, allied to scattered reports of early-onset diabetes in MOPDII (7,8,13), metabolic assessment was undertaken of all other available patients with MOPDII and proven genetic defects in *PCNT* (Table 4). Of 21 patients reviewed, all of whom were under age 30 years, 18 exhibited either fasting hyperinsulinemia or clinical evidence of insulin resistance, including acanthosis nigricans (15 patients). A total of 10 had early-onset diabetes (mean age at diagnosis 15 years [range 5–28]). The three patients who had no evidence of insulin resistance were all under 4 years old, indicating that severe insulin resistance in MOPDII is not congenital but appears during childhood or adolescence. Particularly notable was the observation of an insulin-sensitive boy (patient 4), aged 3 years, with MOPDII who had a 13-year-old sister (patient 12) with the same genotype, MOPDII, and severely insulin-resistant diabetes. Dyslipidemia also was a common feature, with 13 patients for whom data were available showing hypertriglyceridemia and/or low HDL cholesterol. In two patients, clinical and/or biochemical evidence of insulin resistance was first noted during or shortly after growth-hormone therapy. Additional metabolic histories are provided in the Supplementary Materials.

shRNA-mediated knockdown of pericentrin in 3T3-L1 murine preadipocytes. The extreme metabolic syndrome observed in patients with *PCNT* defects closely resembles the deranged metabolism seen in primary forms of lipodystrophy (20) but is unlike the severe insulin resistance with normal lipid profile of patients with insulin receptor defects (15). This led us to hypothesize that loss of pericentrin function may compromise the function of adipose tissue in metabolic homeostasis, either as a result of defective adipogenesis, leading to a state of relative "fat failure," or through a cell-autonomous defect in adipocyte insulin action, associated with defects in proximal insulin signaling or abnormal GLUT4 trafficking. To test these hypotheses, 3T3-L1 preadipocytes were generated, stably expressing shRNA against *Pcnt* (shPcnt1 and shPcnt2) or firefly luciferase as a control (shLuc). shRNA expression reduced *Pcnt* mRNA levels by >70% (Fig. 1*A*) and nearly abolished protein expression (Fig. 1*B*), whereas immunostaining revealed nearly absent centrosomal pericentrin (Fig. 1*C*). Expression of pericentrin mRNA in wild-type, shPcnt1/2, and shLuc cells was assessed throughout the course of adipocyte differentiation. Both wild-type and luciferase knockdown cells showed a consistent doubling of pericentrin expression at day 1, returning to baseline by day 4. Pericentrin expression in knockdown cells was markedly lower than control cells throughout differentiation (Fig. 1*D* and *E*).

Effect of pericentrin knockdown on 3T3-L1 differentiation. Hormonal induction of differentiation in all cell lines resulted in characteristic morphological changes within 24 h, cell proliferation after 36 h, and lipid-droplet appearance after 3 days. By day 8, most control cells contained multiple small lipid droplets. In contrast, differentiation was patchy in knockdown cell lines, with regions of lipid accumulation interspersed with areas devoid of lipid droplets. Oil-Red-O staining of mature adipocytes confirmed that pericentrin knockdown was associated with a marked impairment in triglyceride accumulation

TABLE 4
Metabolic evaluation of patients with proven *PCNT* mutations

Patient number	Sex	Age*	Height (cm)	Weight (kg)	BMI (kg/m^2)	*PCNT* mutation	Fasting glucose (mg/dL)	Fasting insulin (pmol/L)	Triglycerides (mg/dL)	Cholsterol (mg/dL)	HDL (mg/dL)	LDL (mg/dL)	Acanthosis nigricans	Diabetes treatment
3	Female	1.6	52	3.3	12.2	P2353fsX6/P2353fsX6	72.0	11	61.0	139.2	42.5	85.1	No	Nil
4†	Male	3	61	5.4	14.5	E220X/E220X	82.9	18	ND	181.5	ND	ND	No	Nil
5	Male	3	66	5.3	12.2	C1190fs/C1190fs	104.5	161	38.1	108.1	35.5	65.3	NK	Nil
6	Female	3.4	65	5.2	12.3	Q615X/Q1456X	86.0	21	125.0	175.0	46.0	104.0	No	Nil
7	Male	4.5	60.2	5.7	15.7	E348X/E348X	75.7	165	70.8	166.0	ND	ND	No	Nil
8‡	Male	8	103	21.3	20.1	R994fsX60/R994fsX60	122.5	679	946.9	92.3	15.8	107.0	Yes	Metformin
9‡	Female	10	105	20.3	18.4	R994fsX60/R994fsX60	327.9	271	429.2	164.9	17.4	55.0	Yes	Metformin
10	Female	10.5	90.7	11.8	14.3	E2237fsX2244/ E2237fsX2244	192.8	<2	115.0	142.9	48.3	73.4	Yes	CSII
11	Female	12	94.7	16	17.8	IVS1937–1G>CG/ 8048_8049insG (2742X)	108.1	666.72	140.0	171.0	57.0	86.0	Yes	Metformin
2	Female	12	114	25.3	19.5	T2128fsX2129/ T2128fsX2129	84.7	931	362.8	169.9	46.3	50.2	Yes	Metformin
12†	Female	13	96.5	17.5	18.8	E220X/E220X	90.1	623	415.9	262.5	38.6	ND	Yes	Metformin
13	Male	14	84	NK	NK	W2110X/W2110X	88.3	296.1	230.1	135.1	30.9	ND	Yes	Metformin
14	Female	14	99	13.5	13.8	6162_6163hetdelAG (2111X)/ IVS9273+1G>CG	90.1	170	283.2	139.0	35.9	46.3	Yes	Nil
15	Female	14.5	98	20	20.8	E825X/L723fsX9	88.2	416	238.9	169.9	34.0	88.8	Yes	Nil
16	Female	17.2	116	NK	NK	E2756fsX6§	131.5	439	681.4	168.3	26.3	ND	Yes	MDI insulin
17	Female	18	88	12.1	15.6	IVS35+1G>A/ IVS35+1G>A	91.0	109	125.0	170.0	39.0	106.0	No	Nil
18‖	Male	18	97.3	14.5	15.3	Q911QX/R2973RX	34.0	180	271.0	166.0	36.0	76.0	Yes	Nil
19‖	Female	20	69	8.5	17.9	Q911QX/R2973RX	81.0	138	197.0	305.0	73.0	193.0	Yes	Nil
20¶	Male	26	123	30	19.8	D1005fsX1055/ D1005fsX1055	64.9	87	70.8	96.5	32.0	ND	Yes	Nil
21¶	Female	28	116	35	26.0	D1005fsX1055/ D1005fsX1055	189.2	209	238.9	208.5	ND	131.3	Yes	MDI insulin
1	Male	29	111	28.7	23.3	Q1998X/Q3106X	72.1	1990	486.7	251.0	11.2	ND	Yes	Metformin Rosiglitazone Fenoifibrate
Fasting reference range							68–100	<60	<177	<200	>39	<130		

CSII, continuous subcutaneous insulin infusion; MDI, multiple daily injection; ND, not determined; NK, not known; OHA, oral hypoglycemic agent. *Age at time of metabolic evaluation. †, ‡, ‖, and ¶ indicate sibling pairs. §Second mutation not yet confirmed.

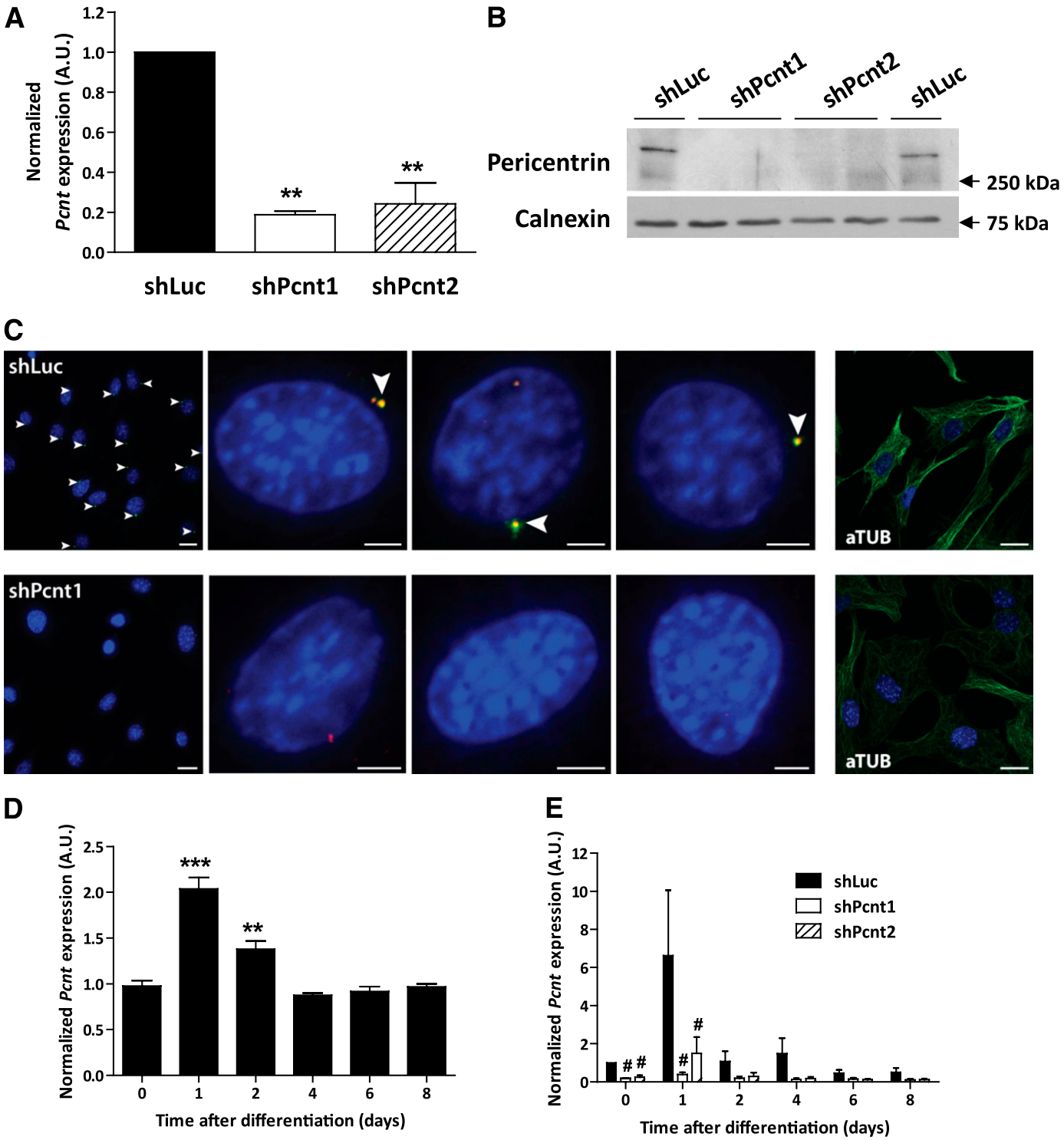

FIG. 1. Stable knockdown of Pcnt in murine 3T3-L1 preadipocytes. *A*: *Pcnt* mRNA expression in shPcnt-infected preadipocytes (□, shPcnt1; ▨, shPcnt2) and luciferase knockdown control preadipocytes (■, shLuc) determined by quantitative real-time PCR. **$P < 0.01$ vs. shLuc ($n = 4$). *B*: Pericentrin expression in shPcnt and shLuc preadipocytes assessed by Western blotting. Calnexin expression was evaluated as a loading control. Representative example of three experiments. *C*: Expression and localization of pericentrin (green), γ-tubulin (red), α-tubulin (green, *far right panels* only), and nuclear material (blue, stained with DAPI) in shPcnt and shLuc preadipocytes, assessed by immunocytochemistry and confocal microscopy. Arrowheads indicate juxtanuclear pericentrin. Scale bars: 20 μm (*far left* and *far right panels*) and 5 μm (*central panels*). *D*: *Pcnt* mRNA expression during differentiation of wild-type 3T3-L1 cells, determined by quantitative real-time PCR. **$P < 0.01$; ***$P < 0.005$ vs. day 0 ($n = 4$). *E*: *Pcnt* mRNA expression during differentiation of shLuc (■) and shPcnt (□ and ▨) preadipocytes. #$P < 0.005$ vs. shLuc ($n = 4$). All data are means ± SE. AU, arbitrary units. (A high-quality digital representation of this figure is available in the online issue.)

(Fig. 2*A*), accompanied by a concomitant mild to moderate (20–40%) defect in the expression of mature adipocyte genes, including *Pparγ2*, *Glut4*, *Fabp4*, *Insr*, and *Acrp30* (Fig. 2*B*). However, the timing of adipocyte gene induction was normal, with early upregulation of *Insr* followed by *Fabp4* and *Glut4* (Supplementary Fig. 5).

Although controversial, evidence has been advanced that two rounds of mitosis (so-called "clonal expansion")

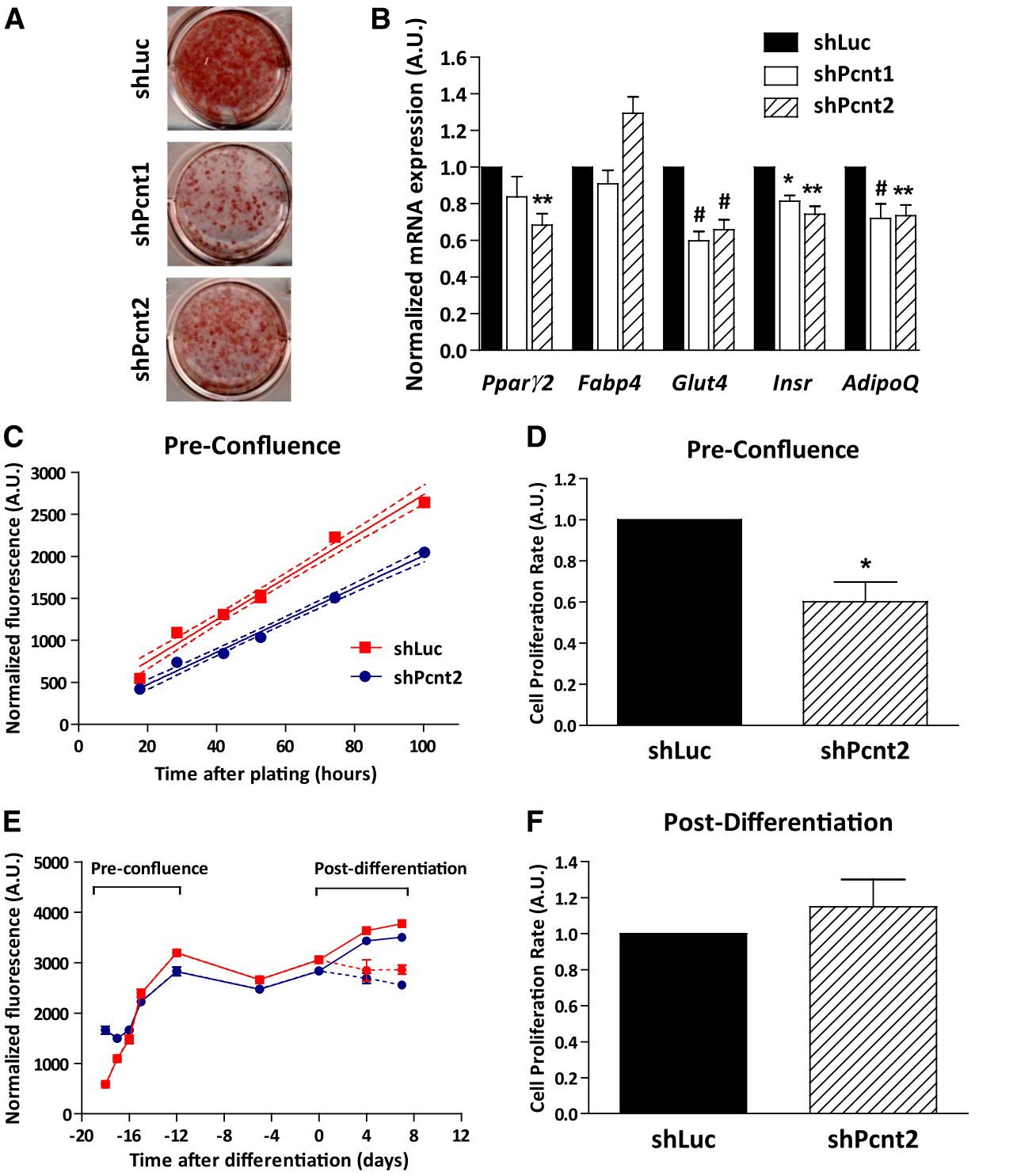

FIG. 2. Pcnt knockdown in 3T3-L1 preadipocytes is associated with impaired adipocyte differentiation. *A*: Oil red O staining of triglycerides at day 10 of differentiation in *Pcnt* knockdown and control adipocytes. Representative of $n = 9$. *B*: Relative adipocyte gene expression in *Pcnt* knockdown (□ and ▨) and control (■) cells at day 10 after differentiation. *$P < 0.05$; **$P < 0.01$; #$P < 0.005$ vs. shLuc ($n = 9$). *C*: Proliferation of shPcnt (blue circles) and control (red squares) preadipocytes during the preconfluent growth phase ($n = 4$). Representative experiments are shown. Data are means ± SE of four wells. *D*: Relative preconfluent rate of proliferation in shPcnt (▨) and control (■) preadipocytes ($n = 3$). *E*: Cell proliferation during the preconfluent phase, confluency, and after hormonal induction of differentiation. Representative experiments are shown. Data are means ± SE of four wells. *F*: Relative rate of cell proliferation after induction of differentiation ($n = 3$). AU, arbitrary units. (A high-quality digital representation of this figure is available in the online issue.)

are a necessary first step in adipogenesis (21). Given the proposed role of pericentrin in mitotic spindle organization, we hypothesized that the differentiation defect resulted from a reduced efficiency of mitosis associated with the absence of pericentrin. As well as displaying a higher frequency of morphological abnormality (not shown), quantification of cell proliferation revealed a significant reduction in preconfluent proliferation of pericentrin

knockdown preadipocytes compared with control cells (Fig. 2*C* and *D*). Cell number at confluence was consistently slightly lower in the knockdown cells. Both cell lines subsequently showed comparable, robust expansion in cell number after induction of differentiation, with a lower final cell number in knockdown cells (Fig. 2*E* and *F*).

Cell-autonomous insulin action after pericentin knockdown. We next tested the hypothesis that severe insulin resistance results from a cell-autonomous defect in insulin signaling, associated with either impaired proximal insulin signaling or GLUT4 translocation. Knockdown of pericentrin had no effect on insulin-stimulated autophosphorylation of its receptor or phosphorylation of two key downstream kinases, protein kinase B (AKT) and extracellular signal–regulated kinase 1/2 (ERK) (Fig. 3*A*). To assess the integrity of the whole signaling pathway from insulin receptor activation to GLUT4 vesicle fusion with the plasma membrane, we next measured insulin-stimulated glucose uptake by differentiated 3T3-L1 adipocytes. Both knockdown and control cells showed a robust, fourfold increase in deoxyglucose uptake, implying that translocation of GLUT4 to the plasma membrane in response to insulin stimulation is intact (Fig. 3*B*). However, both basal and insulin-stimulated glucose uptake were ~50% lower in knockdown compared with control cells, which was approximately commensurate with the degree of impairment in differentiation and argues against any additional cell-autonomous defect in insulin signal transduction in these cells. Consistently, immunostaining of endogenous GLUT4 in mature, unstimulated adipocytes revealed abundant perinuclear GLUT4 with no apparent difference between knockdown and control cell lines (Fig. 3*C*).

Human pericentrin is more abundant in skeletal muscle than any other tissue. To investigate the possible role of nonadipose tissue in metabolic dysregulation in MOPDII, pericentrin mRNA expression was assessed in a range of human tissues. Expression was dramatically higher in skeletal muscle compared with any other tissue, at over 15 times higher than in the brain, which had the second highest expression level, and almost 100 times higher than in white adipose tissue (Fig. 4*A*). The preponderance of pericentrin mRNA expression in human skeletal muscle was not replicated in mouse tissues, where expression was more uniform, with the highest expression in the heart, followed by the pancreas, skeletal muscle, and white adipose tissue (Fig. 4*B*). Immunostaining of human skeletal muscle for pericentrin revealed it to have a perinuclear distribution quite distinct from the punctate centrosomal localization seen in other cell types (Fig. 4*C*). This is consistent with previous studies in murine cells, suggesting that the microtubule organizing center in differentiating myoblasts changes from a punctate to a circumferential structure, with redistribution of pericentrin during this process.

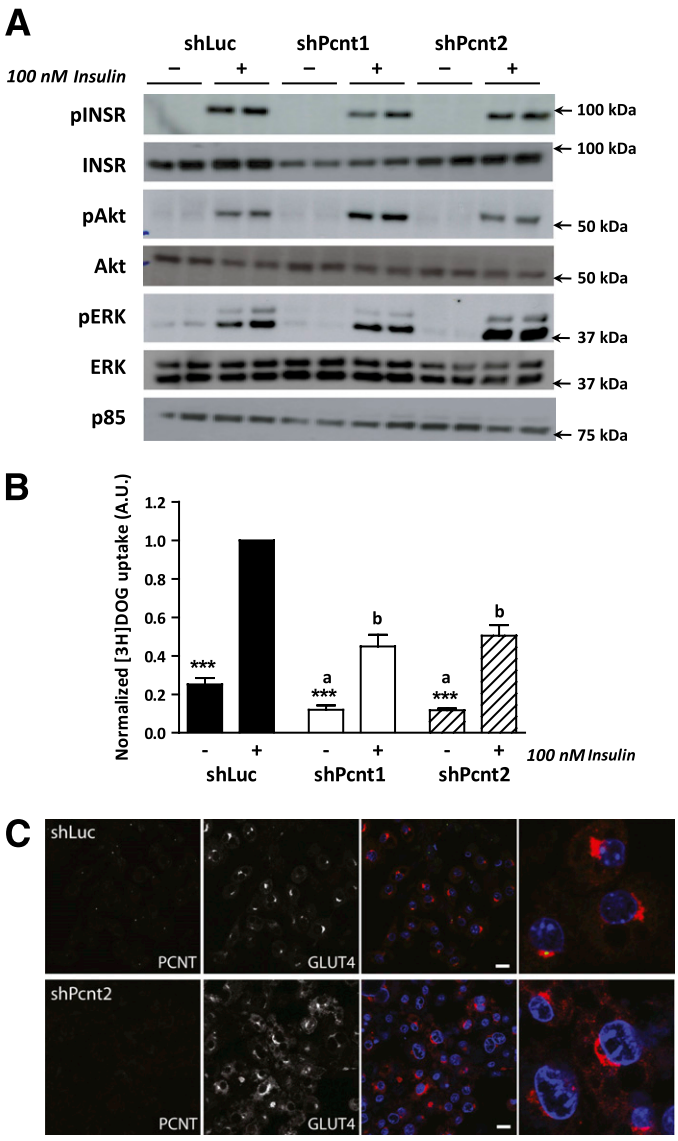

FIG. 3. Knockdown of Pcnt results in mildly impaired insulin-stimulated glucose uptake with normal proximal insulin signaling and GLUT4 localization in adipocytes. *A*: Insulin-stimulated phosphorylation of insulin receptor (INSR), AKT and extracellular signal–regulated kinase (ERK) 1/2 after a 5-min treatment of serum-starved mature adipocytes with 100 nmol/L insulin, assessed by Western blotting. Representative example of three independent experiments. *B*: Relative [^{3}H]deoxyglucose uptake by *Pcnt* knockdown (□ and ▨) and control (■) adipocytes after serum starvation and treatment with 100 nmol/L insulin or PBS for 30 min. ***$P < 0.005$ vs. insulin treatment; $^aP < 0.005$ vs. shLuc after PBS treatment; $^bP < 0.005$ vs. shLuc after insulin treatment. Values are means ± SE ($n = 9$). *C*: Coimmunostaining of pericentrin (green) and endogenous GLUT4 (red) in shLuc (*top panel*) and shPcnt (*bottom panel*) mature adipocytes. *Far right*, magnified image. Blue = DAPI. Scale bar: 5 μm. AU, arbitrary units. (A high-quality digital representation of this figure is available in the online issue.)

DISCUSSION

MOPDII is a rare syndrome of extreme, growth-hormone resistant intrauterine and postnatal growth retardation, characteristic facial dysmorphism, and widespread bone and dental dysplasia (22). Premature death frequently results from intracranial hemorrhage secondary to moya moya–like cerebrovascular abnormalities and intracranial aneurysms (23). Despite severe microcephaly, intelligence is generally normal or only mildly impaired in the absence of cerebrovascular events.

We now report that severe insulin resistance, diabetes, and dyslipidemia are common features of MOPDII associated with *PCNT* mutations. Our observation of infants with *PCNT* mutations and normal insulin sensitivity, including one patient with a severely insulin-resistant 13-year-old sibling, allied to the clinical histories of older patients with severe insulin resistance, suggest that insulin resistance is not congenital but rather becomes manifest most commonly between 5 and 10 years of age. In two cases, insulin resistance was first noted during growth-hormone

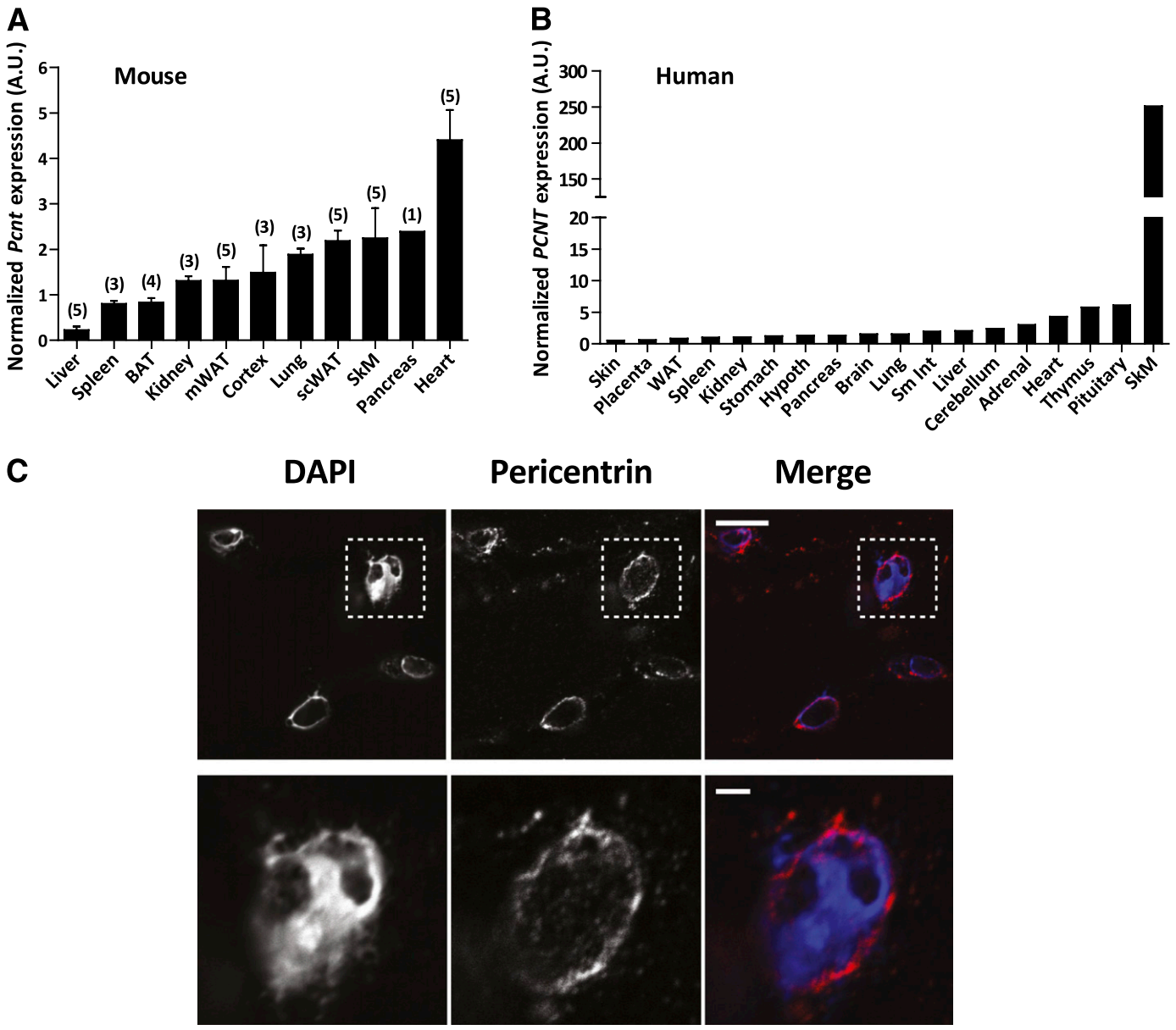

FIG. 4. Pericentrin expression in human and murine tissues. *Pcnt* mRNA expression in a panel of human (*A*) and murine (*B*) tissues determined by quantitative real-time PCR. *A*: Data are means ± SE. Sample sizes are in parentheses. *B*: Data represent *n* = 1. *C:* Immunostaining of pericentrin (red) in human vastus lateralis sections. Nuclei stained with DAPI. *Lower panel* shows magnified images. Scale bars: 5 μm (*top*) and 1 μm (*bottom*). AU, arbitrary units; BAT, brown adipose tissue; Cortex, cerebral cortex; Hypoth, hypothalamus; mWAT, mesenteric white adipose tissue; scWAT, subcutaneous white adipose tissue; SkM, skeletal muscle; SmInt, Small intestine; WAT, white adipose tissue. (A high-quality digital representation of this figure is available in the online issue.)

therapy. MOPDII is not a growth hormone–deficient state, and because growth-hormone therapy is both ineffective in promoting linear growth and is known to exacerbate insulin resistance, we suggest that growth hormone should be avoided in MOPDII.

Although no formal assessment of the prevalence of insulin resistance in MOPDII or PCNT-opathy has been previously conducted, previous reports, including a large case series, attest to the occurrence of acanthosis nigricans, flexural hyperpigmentation worsening with growth-hormone therapy or puberty (hallmarks of acanthosis nigricans), or skin tags in a significant number of patients with a clinical diagnosis of MOPDII (7,8,22). Furthermore, as many as one-third of female patients with MOPDII exhibit precocious puberty, and polycystic ovary syndrome has been confirmed in at least one patient (22). Both precocious puberty and polycystic ovary syndrome are characteristics of severe insulin resistance, although they also have other etiologies. Our finding of highly prevalent severe insulin resistance in those with *PCNT* defects is therefore consistent with earlier clinical reports.

This demonstration that severe insulin resistance is common in MOPDII emphasizes that appropriate and regular surveillance for metabolic disease, including measurements of fasting glucose, lipid profile, and liver function, should be part of the routine management of patients with MOPDII. It also suggests that physiological lessons may be learned from MOPDII as a human "experiment of nature," potentially providing insight into the pathogenic mechanisms behind the complex phenotype of prevalent

insulin resistance. Indeed, patients with *PCNT* defects with severe insulin resistance represent a more faithful model of the metabolic syndrome than patients with insulin receptor defects, who exhibit extreme hyperinsulinemia and ultimately hyperglycemia but are not dyslipidemic and are protected from hepatic steatosis (15). In contrast, patients with *PCNT* defects exhibit not only hyperinsulinemia, which may be extreme, but also are severely dyslipidemic and have hepatic steatosis. Furthermore, although receptoropathy is associated with elevated adiponectin, sex hormone–binding globulin (SHBG), and IGF-binding protein 1 (IGFBP1), all these markers of tissue-specific insulin action are suppressed in the context of *PCNT* loss of function (8). The metabolic phenotype observed in MOPDII therefore mimics, in severe forms, that of morbid obesity or lipodystrophy, each of which may be viewed as examples of adipose failure. Although a centripetal fat distribution is frequently noted in patients with *PCNT* defects, the preservation of adipose tissue on the limbs, total body fat content, and leptin levels collectively rule out frank lipodystrophy. This raises the possibility that pericentrin deficiency may lead to a primary defect in adipocyte insulin action without major impairment of adipose tissue development.

Although complete pericentrin deficiency produces severe insulin resistance and diabetes, the lack of metabolic phenotype in the relatives of patient 1, who are effectively haploinsufficient for pericentrin, argues that a loss of 50% of pericentrin function is insufficient to perturb metabolism and suggests that milder, more common variation in pericentrin expression or function is unlikely to contribute to prevalent forms of insulin resistance and diabetes.

Published data (11) have implicated pericentrin in normal function of the mitotic spindle; it is likely also to help nucleate interphase microtubules. Thus, *PCNT* mutations may impair the generation of adequate numbers of adipocytes at puberty or during growth-hormone therapy as a result of mitotic defects in preadipocytes or mesenchymal stem cells, leading to the production of fewer hypertrophic, unhealthy adipocytes with reduced capacity for energy storage. Here, we have provided evidence in support of this model by demonstrating that knockdown of pericentrin results in impaired cell proliferation, adipogenesis, and triglyceride accumulation in 3T3-L1 preadipocytes, similar to the consequences of knockdown of ALMS1, another large centrosomal protein of unknown function (24). Defects in ALMS1 cause Alström syndrome, which also features severe insulin resistance and dyslipidemia that are disproportionate to adiposity (25,26).

A stoichiometric association of the regulatory subunit of phosphatidyl inositol 3-kinase with the centrosome in response to insulin action has been reported, suggesting that the centrosome may play a role in early events in insulin signal transduction (27). *PCNT* defects also lead to deranged microtubule architecture, which might be expected to perturb intracellular localization and trafficking of GLUT4 vesicles within adipocytes. However, we found no evidence of a defect in either proximal insulin signaling or in insulin-stimulated glucose uptake after pericentrin knockdown in 3T3-L1 preadipocytes.

It remains to be determined whether the mild differentiation defect caused by loss of *PCNT* expression in preadipocytes is sufficient to account for severe insulin resistance in vivo. Indeed, the severity of insulin resistance in MOPDII, which is at least as great as that in congenital generalized lipodystrophy, suggests that other factors may be at play. Our finding of highly abundant pericentrin in human skeletal muscle raises the possibility that it may be involved in muscle insulin action. Despite the extremely high expression of pericentrin in skeletal muscle, however, patients with *PCNT* defects show no clinical evidence of myopathy. Moreover, no cellular models reliably recapitulate insulin-stimulated, GLUT4-mediated glucose uptake, precluding in vitro study in this case; future in vivo studies are therefore required.

One recent report (28) using cultured cells and mice transplanted with pancreatic islets with or without pericentrin knockdown suggested that pericentrin deficiency may lead to insulin hypersecretion in the fasting state, with reduced ability to clear a glucose load. However, our human observations show unequivocal and severe insulin resistance, with neither clinical nor biochemical evidence of antecedent hypoglycemia. Furthermore, although high levels of insulin may lead to insulin receptor downregulation, there are no reported precedents for primary insulin hypersecretion as a cause of severe systemic insulin resistance. Collectively, these observations argue against dysregulation of insulin secretion as the dominant defect underlying insulin-resistant diabetes in MOPDII.

In summary, we establish that MOPDII, a syndrome of primordial dwarfism attributed to loss of function of pericentrin, also encompasses severe insulin resistance, diabetes, and dyslipidemia. This appears to manifest most commonly between age 5 and 15 years and may be unmasked by growth-hormone therapy. Equivalent loss of pericentrin in vitro leads to impaired adipocyte differentiation with commensurately reduced insulin-stimulated glucose uptake, possibly secondary to impaired preadipocyte proliferation. Additional elucidation of the mechanisms whereby defects in pericentrin lead to insulin resistance in vivo may not only enhance understanding of this rare condition but also may offer insights into the pathogenesis of common insulin resistance.

ACKNOWLEDGMENTS

Support was provided by the U.K. Medical Research Council, Centre for Obesity and Related Disorders, and the National Institute for Health Research, Cambridge Biomedical Research Centre. I.H.-D. is supported by the Sackler Fund for Medical Science and the James Baird Fund. R.K.S. and S.O'R. are supported by the Wellcome Trust (Intermediate Clinical Fellowship 080952/Z/06/Z and Programme Grant no. 078986/Z/06/Z). L.S.B. and A.P.J. are supported by a Medical Research Council Senior Clinical Fellowship.

No potential conflicts of interest relevant to this article were reported.

I.H.-D. wrote the manuscript. L.S.B. reviewed and edited the manuscript. I.H.-D. and L.S.B. researched data and contributed to discussion. F.M.F. researched data and reviewed and edited the manuscript. N.R., K.M.P., Y.C.L.T., and F.S. researched data. A.K. researched data, contributed to discussion and reviewed and edited the manuscript. J.J.N. and M.O'D. researched data and reviewed and edited the manuscript. M.B. researched data, contributed to discussion, and reviewed and edited the manuscript. S.O'R. contributed to discussion and reviewed and edited the manuscript. A.P.J. researched data, contributed to discussion, and reviewed and edited the manuscript. R.K.S. researched data, contributed to discussion, and wrote the manuscript. All clinicians listed under the MOPD II

Study Group researched data and reviewed and edited the manuscript.

The authors are grateful to all participating patients and to those additional referring clinicians, including Professor Yanick Crow (University of Manchester and the Manchester Academic Health Science Centre, Manchester, U.K.), Dr. Dorota Birkholz (University of Gdańsk, Gdańsk, Poland), and Dr. Francisca Ugarte (Hospital Exequiel González Cortés, Santiago, Chile).

APPENDIX

Members of the MOPD Study Group: Nouriya Al Sannaa, Pediatrics Services Division, Dhahran Health Center, Saudi Aramco Medical Services Organization, Dhahran, Saudi Arabia; Sabah Alvi, Leeds General Infirmary, Leeds, U.K.; Rakesh Amin, Barts and The London Children's Hospital, London, U.K.; Krystyna H. Chrzanowska, Department of Medical Genetics, The Children's Memorial Health Institute, Warsaw, Poland; Bruno Dallapiccola, IRCCS-CSS, San Giovanni Rotondo and CSS-Mendel Institute, Rome, and the Department of Experimental Medicine and Pathology, University of Rome La Sapienza, Rome, Italy; James Greening, Department of Pediatrics, Leicester Royal Infirmary, Leicester, U.K.; Ben Hamel, Department of Human Genetics, Radboud University Nijmegen Medical Center, Nijmegen, the Netherlands; Katerina K. Harwood, St. Joseph Hospital and Medical Centre, Paterson, New Jersey; Elena Hennessy, Endocrinology Research Centre, Institute of Pediatric Endocrinology, Moscow, Russia; Celine Huot, Centre Hospitalier Universitaire Sainte-Justine, Centre de Recherche, Montréal, Québec, Canada; Anita Rauch, Institute of Medical Genetics, University of Zurich, Schwerzenbach, Switzerland; Gabriela Repetto, Centre for Human Genetics, Faculty of Medicine, Clínica Alemana-Universidad del Desarrollo, Santiago, Chile; Joao Silva, Medical Genetics Unit, Jacinto Magalhaes Centre for Medical Genetics, Dr. Ricardo Jorge, National Institutes of Health, Porto, Portugal; Natalia Volevodz, Endocrinology Research Centre, Institute of Pediatric Endocrinology, Moscow, Russia.

REFERENCES

1. Reaven GM. Pathophysiology of insulin resistance in human disease. Physiol Rev 1995;75:473–486
2. Lee JM, Okumura MJ, Davis MM, Herman WH, Gurney JG. Prevalence and determinants of insulin resistance among U.S. adolescents: a population-based study. Diabetes Care 2006;29:2427–2432
3. Kahn SE, Hull RL, Utzschneider KM. Mechanisms linking obesity to insulin resistance and type 2 diabetes. Nature 2006;444:840–846
4. Dupuis J, Langenberg C, Prokopenko I, et al. New genetic loci implicated in fasting glucose homeostasis and their impact on type 2 diabetes risk. Nat Genet 2010;42:105–116
5. Rung J, Cauchi S, Albrechtsen A, et al. Genetic variant near IRS1 is associated with type 2 diabetes, insulin resistance and hyperinsulinemia. Nat Genet 2009;41:1110–1115
6. Altshuler D, Hirschhorn JN, Klannemark M, et al. The common PPARgamma Pro12Ala polymorphism is associated with decreased risk of type 2 diabetes. Nat Genet 2000;26:76–80
7. Griffith E, Walker S, Martin CA, et al. Mutations in pericentrin cause Seckel syndrome with defective ATR-dependent DNA damage signaling. Nat Genet 2008;40:232–236
8. Rauch A, Thiel CT, Schindler D, et al. Mutations in the pericentrin (PCNT) gene cause primordial dwarfism. Science 2008;319:816–819
9. Dictenberg JB, Zimmerman W, Sparks CA, et al. Pericentrin and gamma-tubulin form a protein complex and are organized into a novel lattice at the centrosome. J Cell Biol 1998;141:163–174
10. Doxsey SJ, Stein P, Evans L, Calarco PD, Kirschner M. Pericentrin, a highly conserved centrosome protein involved in microtubule organization. Cell 1994;76:639–650
11. Zimmerman WC, Sillibourne J, Rosa J, Doxsey SJ. Mitosis-specific anchoring of gamma tubulin complexes by pericentrin controls spindle organization and mitotic entry. Mol Biol Cell 2004;15:3642–3657
12. Diviani D, Langeberg LK, Doxsey SJ, Scott JD. Pericentrin anchors protein kinase A at the centrosome through a newly identified RII-binding domain. Curr Biol 2000;10:417–420
13. Willems M, Genevieve D, Borck G, et al. Molecular analysis of pericentrin gene (PCNT) in a series of 24 Seckel/microcephalic osteodysplastic primordial dwarfism type II (MOPD II) families. J Med Genet 2010;47:797–802
14. Andersen L, Dinesen B, Jørgensen PN, Poulsen F, Røder ME. Enzyme immunoassay for intact human insulin in serum or plasma. Clin Chem 1993;39:578–582
15. Semple RK, Sleigh A, Murgatroyd PR, et al. Postreceptor insulin resistance contributes to human dyslipidemia and hepatic steatosis. J Clin Invest 2009;119:315–322
16. Semple RK, Soos MA, Luan J, et al. Elevated plasma adiponectin in humans with genetically defective insulin receptors. J Clin Endocrinol Metab 2006;91:3219–3223
17. Rochford JJ, Semple RK, Laudes M, et al. ETO/MTG8 is an inhibitor of C/EBPbeta activity and a regulator of early adipogenesis. Mol Cell Biol 2004;24:9863–9872
18. George S, Johansen A, Soos MA, et al. Deletion of V335 from the L2 domain of the insulin receptor results in a conformationally abnormal receptor that is unable to bind insulin and causes Donohue's syndrome in a human subject. Endocrinology 2003;144:631–637
19. Al-Khalili L, Chibalin AV, Kannisto K, et al. Insulin action in cultured human skeletal muscle cells during differentiation: assessment of cell surface GLUT4 and GLUT1 content. Cell Mol Life Sci 2003;60:991–998
20. Garg A. Acquired and inherited lipodystrophies. N Engl J Med 2004;350:1220–1234
21. Tang QQ, Otto TC, Lane MD. Mitotic clonal expansion: a synchronous process required for adipogenesis. Proc Natl Acad Sci USA 2003;100:44–49
22. Hall JG, Flora C, Scott CI Jr, Pauli RM, Tanaka KI. Majewski osteodysplastic primordial dwarfism type II (MOPD II): natural history and clinical findings. Am J Med Genet A 2004;130A:55–72
23. Brancati F, Castori M, Mingarelli R, Dallapiccola B. Majewski osteodysplastic primordial dwarfism type II (MOPD II) complicated by stroke: clinical report and review of cerebral vascular anomalies. Am J Med Genet A 2005;139:212–215
24. Huang-Doran I, Semple R. Knockdown of the Alstrom syndrome-associated gene Alms1 in 3T3-L1 preadipocytes impairs adipogenesis but has no effect on cell autonomous insulin action. Int J Obes 2010;34:1554–1558
25. Marshall JD, Beck S, Maffei P, Naggert JK. Alström syndrome. Eur J Hum Genet 2007;15:1193–1202
26. Minton JA, Owen KR, Ricketts CJ, et al. Syndromic obesity and diabetes: changes in body composition with age and mutation analysis of ALMS1 in 12 United Kingdom kindreds with Alstrom syndrome. J Clin Endocrinol Metab 2006;91:3110–3116
27. Kapeller R, Toker A, Cantley LC, Carpenter CL. Phosphoinositide 3-kinase binds constitutively to alpha/beta-tubulin and binds to gamma-tubulin in response to insulin. J Biol Chem 1995;270:25985–25991
28. Jurczyk A, Pino SC, O'Sullivan-Murphy B, et al. A novel role for the centrosomal protein, pericentrin, in regulation of insulin secretory vesicle docking in mouse pancreatic beta-cells. PLoS ONE 2010;5:e11812
29. Borrud LG, Flegal KM, Looker AC, Everhart JE, Harris TB, Shepherd JA. Body composition data for individuals 8 years of age and older: U.S. population, 1999-2004. Vital Health Stat 11 2010;(250):1–87